next-gen knowledge

stay up-to-date with
the latest technology

ATTENDEE PROGRAM

OFC

The future of optical networking
and communications

TECHNICAL CONFERENCE
11 – 15 March 2018

EXHIBITION
13 – 15 March 2018

San Diego, California, USA

ofcconference.org

SPONSORED BY:
IEEE ComSoc IEEE Communications Society
IEEE photonics Society
OSA The Optical Society | 100 Since 1916
Managed by OSA

Agenda of Sessions — Thursday, 15 March

	Room 1A	Room 1B	Room 2	Room 6C ▶	Room 6D ▶	Room 6E ▶	Room 6F ▶
07:30–08:00	**Coffee Break,** *Upper Level Corridors*						
08:00–10:00	**Th1A • Advances in Coherent Design and Measurement**	**Th1B • 5G Transport** (begins at 08:30)	**Th1C • Wideband Transmission** (begins at 09:00)	**Th1D • Application Awareness and Online Optimization** ▶	**Th1E • Components for Future PON** ▶	**Th1F • High Capacity Subsystems** ▶	**Th1G • Photonic Networks for Data Centers** ▶ (begins at 08:15)
10:00–16:00	**Exhibition and Show Floor Programs, Coffee Break,** *Exhibit Hall* **and OFC Career Zone Live,** *Exhibit Hall C*						
10:30–12:30	**Th2A • Joint Poster Session II,** *Exhibit Hall B*						
12:30–14:00	**Unopposed Exhibit-only Time,** *Exhibit Hall* (concessions available)						
14:00–16:00	**Th3A • Current Topics in Long Haul/ Metro Transmisssion** (ends at 15:00)			**Th3B • Directly Modulated Lasers** ▶	**Th3C • Optical Switching II** ▶	**Th3D • Nonlinear Fiber Effects** ▶	**Th3E • Advanced Transmission Technology** ▶ (ends at 15:45)
16:00–16:30	**Beverage and Coffee Break,** *Upper Level Corridors*						
16:30–18:30	**Postdeadline Sessions,** *Rooms 6C, 6D, 6E, 6F*						

Key to Shading

■ Market Watch/Network Operator Summit ▶ Recorded Session

10:30–12:30
Th2A • Joint Poster Session II

Th2A.1
O-band Silicon Photonics 8×8 Arrayed Waveguide Grating Router (AWGR) for 1.6 Tb/s On-chip Routing, Stelios Pitris[1,2], George Dabos[1,2], Charoula Mitsolidou[1,2], Theoni Alexoudi[1,2], Peter De Heyn[3], Joris Van Campenhout[3], Ronald Broeke[4], George T. Kanellos[5], Nikos Pleros[1,2]; *[1]Department of Informatics, Aristotle Univ. of Thessaloniki, Greece; [2]Center for Interdisciplinary Research and Innovation, Aristotle Univ. of Thessaloniki, Greece; [3]imec, Belgium; [4]Bright Photonics BV, Netherlands; [5]High Performance Networks Group, Univ. of Bristol, UK.* We present an 8×8 silicon photonics AWGR with 10 nm channel spacing for O-band cyclic-routing operation. Successful transmission at 25 Gb/s is demonstrated for all 8×8 AWGR channel combinations with a maximum power penalty of 0.82 dB.

Th2A.2
Poly-crystalline Silicon Waveguide Devices on Hollow Deep Trench Isolation in Standard Foundry Bulk Silicon Process, Sungwon Chung[1], Makoto Nakai[1], Edward Preisler[2], Hossein Hashemi[1]; *[1]Univ. of Southern California, USA; [2]TowerJazz, USA.* We first demonstrate poly-crystalline silicon waveguide devices on deep-trench isolation in a commercial bulk 180nm SiGe BiCMOS process without any process modifications or post-processing. At 1550nm, the measured loss for the poly-crystalline silicon waveguide and an MMI compatible with the waveguide are around 3.0 dB/mm and 0.38 dB, respectively.

Th2A.3
Integrated InP Polarization Rotator Using the Plasmonic Effect, Shinmo An[1], O-Kyun Kwon[1]; *[1]ETRI, Korea.* An InP based polarization rotator is demonstrated using the plasmonic effect. It operates as a half-wave retarder. Simple device structure ensures large fabrication tolerance. The device exhibits polarization extinction ratio of 20 dB over C-band.

Th2A.4
Thermo-optical Phase Shifter with Integrated Diodes for Multiplexed Control, Antonio R. Alves[1,2], Wim Bogaerts[1,2]; *[1]Ghent Univ. - IMEC, Photonics Research Group, Belgium; [2]Center for Nano and Biophotonics (NB-photonics), UGent, Belgium.* We present a thermo-optic silicon phase shifter with diodes for multiplexed control and demonstrate that such heaters can be driven using digital signals to increases the linearity of the phase shift response of the device.

Th2A.5
Integrated Polarization Beam Splitter Module for Polarization-encoded Free-space BB84 QKD, Joong-Seon Choe[1], Heasin Ko[1], Byung-Seok Choi[1], Kap-Joong Kim[1], Chun Ju Youn[1]; *[1]ETRI, Korea.* We present an integrated polarization beam splitter module for free-space BB84 quantum key distribution. The module is based on silica PLC birefringent Mach-Zehnder interferometer chip, and replaces successfully the bulk-optic-based polarization splitting subsystem of BB84 quantum key distribution test-bed operating at 780 nm.

Th2A.6
Compact Grating Coupler for Higher-order Mode Coupling, Yaxiao Lai[1], Yu Yu[1], Songnian Fu[1], Jing Xu[1], Perry Ping Shum[2], Xinliang Zhang[1]; *[1]Wuhan National Lab for Optoelectronics, China; [2]School of Electrical and Electronics Engineering, Nanyang Technological Univ., Singapore.* An on-chip LP_{11}-tE_1 mode grating coupler is experimentally demonstrated by utilizing double-grating structure and a Y-junction. A 0.6 dB improvement of coupling efficiency with a quarter taper length is achieved comparing with conventional grating coupler.

Th2A.7
Compact and Power Efficient 2 × 2 Thermo-optical Switch based on Dual-nanobeam MZI, Jiang Xinhong[1], Hongxia Zhang[1], Ciyuan Qiu[1], Yong Zhang[1], Yikai Su[1], Richard A. Soref[2]; *[1]Shanghai Jiao Tong Univ., China; [2]Univ. of Massachusetts, USA.* A compact 2×2 thermo-optical switch based on a dual-nanobeam MZI is experimentally demonstrated. The footprint is 38 μm×84 μm. The heating powers for the cross and bar states are ~2.66 mW and ~2.36 mW, respectively.

Th2A.8
Broadband SOI Mode Order Converter based on Topology Optimization, Min Teng[1,2], Keisuke Kojima[1], Toshiaki Koike-Akino[1], Bingnan Wang[1], Chungwei Lin[1], Kieran Parsons[1]; *[1]Mitsubishi Electric Research Labs, USA; [2]Purdue Univ., USA.* Topology optimized SOI mode order converters are proposed to allow mutual conversion between TE_0, TE_1 and TE_2. Broadband conversion efficiency around 85% can be realized on an ultra-compact (~ 4 μm) footprint.

Th2A.9
Design, Fabrication and Demonstration of Ultra-broadband Orbital Angular Momentum (OAM) Modes Emitter and Synthesizer on Silicon Platform, Zhou Nan[1], Shuang Zheng[1], Xiaoping Cao[1], Shengqian Gao[2], Shimao Li[2], Mingbo He[2], Jian Wang[1], XinLun Cai[2]; *[1]Wuhan National Laboratory for Optoelectr, China; [2]State Key Laboratory of Optoelectronic Materials and Technologies and School of Physics and Engineering, Sun Yatsen Univ., China.* We design, fabricate and demonstrate chip-scale ultra-broadband orbital angular momentum (OAM) emitter and synthesizer on a silicon platform. The maximum purity of OAM_{+1} and synthesized OAM_{+1} and OAM_{-1} are 0.93 and 0.9 in telecommunication band.

Th2A.10
Ultra-compact Silicon Polarization Beam Splitter with a Short Coupling Length of 0.768 μm, Yong Zhang[1], Xiaodong Wang[1], Xuhan Guo[1], Ciyuan Qiu[1], Xiulan Cheng[1], Yikai Su[1], Richard A. Soref[2]; *[1]Shanghai Jiao Tong Univ., China; [2]Univ. of Massachusetts, USA.* We demonstrate an ultra-compact silicon polarization beam splitter with a coupling length of 0.768 μm. Lower than 2-dB insertion losses and over 10-dB extinction ratios are achieved over a wavelength range of 60 nm.

Th2A.11
Inter-die Fabrication Uniformity of Silicon Photonic Fiber-to-waveguide Edge Couplers, Junrong Ong[1], Thomas Ang[1], Xin Guo[2], Ezgi Sahin[3], Soon Thor Lim[1], Dawn Tan[3], Wang Hong[2], Ching Eng, Jason Png[1]; *[1]Inst. of High Performance Computing , Singapore; [2]Nanyang Technological Univ., Singapore; [3]Singapore Univ. of Technology and Design, Singapore.* Silicon-on-insulator fiber-to-waveguide inverse taper edge couplers of different tip widths of 120nm to 200nm are fabricated using a multi-project wafer service. The coupling efficiencies and the inter-die fabrication uniformity of the edge couplers are compared.

Th2A.12
A Simple, Robust Two- tone Method to Measure the Dynamic Nonlinear Characteristics of Phase Shifter in Silicon Mach-Zehnder Modulator, Tong Ye[1], Yanhui Qi[1], Hao Chen[1], Zhenning Tao[1], Tomofumi Oyama[2], Hisao Nakashima[2], Takeshi Hoshida[2], Haowen Shu[3], Xingjun Wang[3]; *[1]Fujitsu R&D Center, China; [2]Fujitsu Laboratories Ltd, Japan; [3]Peking Univ., China.* A simple and robust method is proposed to measure high-frequency nonlinear phase-voltage relationship of phase shifter in silicon Mach-Zehnder modulator. Experiments show that static and dynamic characteristics are different, and nonlinearity decreases along with frequency.

Th2A.13
A Large-signal Equivalent Circuit for Depletion-type Silicon Ring Modulators, Minkyu Kim[1], Myungjin Shin[1], Min-Hyeong Kim[1], Byung-Min Yu[1], Christian Mai[2], Stefan Lischke[2], Lars Zimmermann[2], Woo-Young Choi[1]; *[1]Yonsei Univ., Korea; [2]IHP, Germany.* We demonstrate an accurate and easy-to-use large-signal equivalent circuit for depletion-type Si ring modulators. Design optimization of a 25-gbps Si photonic transmitter including the driver and the modulator is carried out entirely with SPICE simulation.

Th2A.14
Narrow Linewidth Hybrid InP-triPleX Photonic Integrated Tunable Laser based on Silicon Nitride Micro-ring Resonators, Yi Lin[1], Colm Browning[1], Roelof Bernardus Timens[2], Douwe H. Geuzebroek[2], Chris G. H. Roeloffzen[2], Dimitri Geskus[2], Ruud M. Oldenbeuving[2], René G. Heideman[2], Youwen Fan[3,2], Klaus J. Boller[3], Jialin Zhao[4], Liam Barry[1]; *[1]Dublin City Univ., Ireland; [2]LioniX International, Netherlands; [3]Univ. of Twente, Netherlands; [4]Huawei Technologies Co., China.* Detailed characterization of a hybrid integrated tunable laser based on micro-ring resonators shows a tuning range of 50 nm with ~40 kHz linewidth. The device demonstrates performance comparable with commercial external cavity lasers in 16QAM coherent system.

Th2A.15
High Performance Self-injection Locked 524 nm Green Laser Diode for High Bitrate Visible Light Communications, Md. Hosne Mobarok Shamim[1], Mohamed Shemis[1], Chao Shen[2], Hassan Oubei[2], Tien K. Ng[2], Boon Ooi[2], Mohammed Z. Khan[1]; *[1]Electrical Engineering, King Fahd Univ. of Petroleum & Minerals, Saudi Arabia; [2]King Abdullah Univ. of Science and Technology, Saudi Arabia.* First demonstration of self-injection locking on 524 nm visible laser diode is presented. Enhancement by ~440 MHz (~30%) in modulation bandwidth, ~7 times reduction in lasing linewidth, and ~10 dB improvement in SMSR is achieved.

Th2A.16
High Throughput Bandwidth Characterization of Silicon Photonic Modulators using Offset Frequency Combs, Nathan Abrams[1], Robert Polster[1], Liang Y. Dai[1], Keren Bergman[1]; *[1]Columbia Univ., USA.* We develop a low complexity, high-throughput testing technique for concurrently characterizing the bandwidths of multiple in-series modulators with independent frequency combs. The approach is demonstrated on two serial modulators at 9.2 GHz and 15.5 GHz.

Th2A.17
Phase Noise Characterization of a Mode-locked Quantum-dot Coherent Optical Frequency Comb Source Laser, Kristian Zanette[1], John C. Cartledge[1], Rongqing Hui[3], Maurice O'Sullivan[2]; *[1]Queen's Univ. at Kingston, Canada; [2]Ciena, Canada; [3]Univ. of Kansas, USA.* The amplitude fluctuations and correlation times of the two contributions to the phase noise of a quantum-dot optical frequency comb source laser are characterized using simultaneously recovered phase noise trajectories for pairs of comb lines.

Th2A.18
A 520-nm Green GaN LED with High Bandwidth and Low Current Density for Gigabits OFDM Data Communication, Chien Ju Chen[1], Jhih-Heng Yan[2], De-Hua Chen[3], Kai-Hsiang Lin[2], Kai Ming Feng[2,3], Meng Chyi Wu[1,3]; *[1]Inst. of Electronics Engineering, National Tsing Hua Univ., Taiwan; [2]Inst. of Communications Engineering, National Tsing Hua Univ., Taiwan; [3]Inst. of Photonics Technologies, National Tsing Hua Univ., Taiwan.* We develop 520-nm green GaN LEDs with a 340-mHz E-o bandwidth. For the first time, an OFDM signal modulates the green LED, which data rate achieves 2.16 Gb/s at a low current density 679 A/cm^2.

A Large-signal Equivalent Circuit for Depletion-type Silicon Ring Modulators

Minkyu Kim, Myungjin Shin, Min-Hyeong Kim, Byung-Min Yu, Christian Mai[+], Stefan Lischke[+], Lars Zimmermann[+] and Woo-Young Choi

Department of Electrical and Electronic Engineering, Yonsei University, Seoul Korea
[+]IHP, Im Technologiepark 25, 15236 Frankfurt (Oder), Germany
minkyu226@yonsei.ac.kr

Abstract: We demonstrate an accurate and easy-to-use large-signal equivalent circuit for depletion-type Si ring modulators. Design optimization of a 25-Gbps Si photonic transmitter including the driver and the modulator is carried out entirely with SPICE simulation.

OCIS codes: (130.4110) Modulators; (230.5750) Resonators; (250.3140) Integrated optoelectronic circuits.

1. Introduction

Depletion-type Si ring modulators (RMs) attract a great amount of research interests since they can provide such advantages for optical interconnect applications as large modulation bandwidth and small-footprint [1, 2]. For realizing Si electronic-photonic integrated circuits that include Si RMs, Si RM models are needed that are accurate, easy-to-use, and compatible with the standard IC design tools. In addition, extracting numerical values for model parameters should be simple and straight-forward. A precise analytical model for the Si RM was reported [3] but it is not compatible with Si IC design tools and requires more than 10 parameters for accurate results. In [4], the coupled-mode description of the Si RM was implemented in Verilog-A, but it requires a substantial amount of computation time since Verilog-A is not optimized for numerically solving differential equations and a very fine time resolution is needed for accurate description of the Si RM dynamics.

In this paper, we present an entirely new approach based on the linear equivalent circuit of the Si RM [5], which contains only four independent model parameters that can be easily extracted from simple RM transmission measurement. Although model parameter values nonlinearly depend on the Si RM bias voltage, we demonstrate that, by using voltage-dependent circuit elements available within SPICE model, large-signal transient modulation characteristics can be easily and accurately simulated with at least 220 times smaller simulation time compared to the approach used in [4]. Such reduction in computation time should provide a great advantage for design optimization of high-performance Si photonic interconnects that contain many Si RMs as well as various electronic circuit blocks.

2. Large-signal Equivalent Circuit

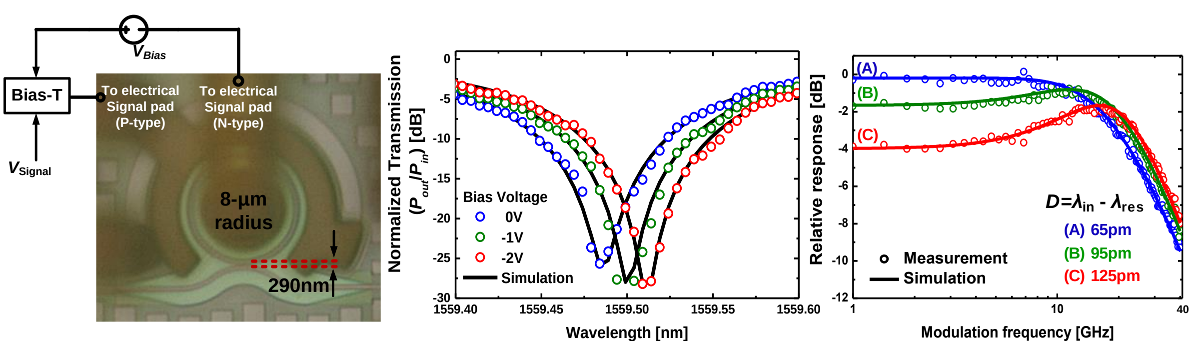

(a) (b) (c)

Fig. 1(a) Chip photo of a fabricated Si RM, (b) Measured and simulated transmission characteristics of Si MRM for different V_{Bias} and (c) Measured and calculated E/O frequency responses for three detuning values.

Fig. 1(a) shows the chip photo of a depletion-type Si RM used for our investigation. The device is fabricated by Si photonics foundry provided by IHP. Empty circles in Fig. 1(b) show the measured normalized transmission characteristics at three different bias voltages. The numerical values for three key model parameters (n_{eff} for the ring waveguide effective index, τ and τ_l for the decay time constant of the energy amplitude in the coupled and the uncoupled ring resonator, respectively [6]) can be extracted by fitting the model to the measured transmission. Solid lines in Fig. 1(b) show the fitted results with extracted values given in Table I. With these and the detuning parameter (D), indicating how much the input light angular frequency is detuned from the resonance angular frequency, the Si RM small-signal modulation frequency response characteristics can be described in the s-domain as [5]

$$G \cdot \frac{s + 2/\tau_l}{s^2 + (2/\tau)s + D^2 + 1/\tau^2}, \quad (1)$$

where G is a function of n_{eff}, τ, τ_l and D. Fig. 1(c) shows the comparison between measured and calculated Si RM E/O frequency responses at three different D values given in wavelength.

Fig. 2(a) shows the large-signal equivalent circuit for the Si RM. It contains a block for parasitic components due to interconnects and pads, another for the electrical elements of the core p-n junction (R_s and C_j), and the third for a lossy LC tank emulating the Si MRM small-signal modulation frequency response given in (1). Numerical values for the parasitic components as well as R_s and C_j can be easily determined by the standard electrical s-parameter measurement. Numerical values for R_1, R_2, C and L are determined from τ_l, τ and D. g is a unit-converting scaling factor.

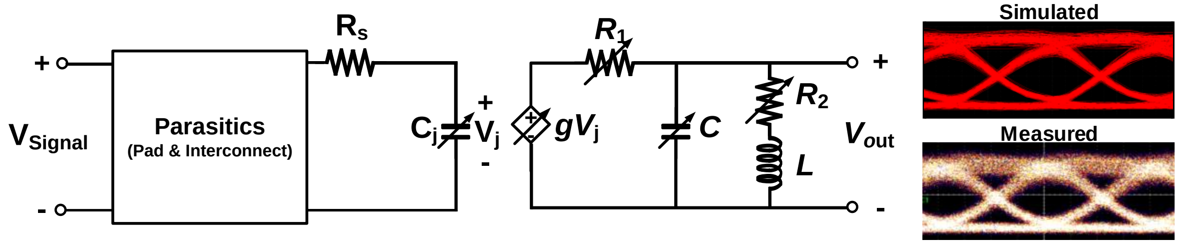

Fig. 2(a) A large-signal equivalent circuit model of Si MRM
and (b) Simulated (upper) and measured (lower) eye-diagrams for 2-Vpp, 25-Gbps, 2^{31}-1 PRBS input signal.

TABLE I: EXTRACTED PARAMETER VALUES

V_{Bias} (V)	n_{eff}	τ_l (ps)	τ (ps)
0	2.637124	22.42	11.74
-1	2.637150	22.88	11.86
-2	2.637167	23.12	11.93

TABLE II: EQUIVALENT CIRCUIT PARAMETERS

V_{Bias} (V)	R_s (Ω)	C_j (fF)	R_1 (Ω)	C (fF)	R_2 (KΩ)	L (nH)
0	365.5	12	3065	4.01	10.20	114.41
-1		8.2	1725	7.13	10.00	
-2		6.5	1016	12.12	9.90	

In this circuit, C_j, R_1, R_2, C are voltage-dependent nonlinear elements, which can be easily handled with the standard circuit simulators. Table II shows numerical values for these circuit parameters at three different bias voltages, all of which are calculated form the values given in Table I. Using this circuit model, we simulated Si RM eye-diagrams in Synopsys HSPICE (Version M 2017.03). Although parameter values at only three different biases are given, the simulator automatically interpolates the values at a given bias voltage. Fig. 2(b) shows the simulated eye-diagram (upper) and the measured result (lower), confirming the accuracy of our model. For simulation and measurement, the Si RM is driven with 25-Gbps $2^{31}-1$ PRBS having 2-$V_{peak\text{-}to\text{-}peak}$. For input wavelength, D = 40 pm at the reverse bias voltage of 1 V. For 1-μs long transient simulation with 0.1ps time step, the approach reported in [4] requires 980 seconds whereas our new approach needs only 4.43 s in our simulation environment.

3. Co-simulation of Si RM and BiCMOS driver

The real advantage of our model is the ease with which it can be used for co-simulation of electronic circuits and Si RMs. Fig. 3(a) shows a schematic diagram for an integrated 25-Gbps Si photonic transmitter containing a fully differential cascode common-emitter driver and a Si RM. Such an electronic-photonic integrated circuit can be fabricated monolithically with IHP's Photonic BiCMOS technology, which provides high-performance 0.25-μm SiGe BiCMOS circuits and Si photonic components on the same Si platform [7]. With our model, the design optimization of the entire transmitter can be easily carried out. Fig. 3(b) shows the simulated vertical eye opening normalized to input optical power at different values of I_{tail} and R_L, two key parameters in the driver that determine eye-opening, power consumption, and bandwidth. For the simulation, 25-Gbps $2^{31}-1$ PRBS data are supplied between V^{+}_{in} and V^{-}_{in}. These results clearly point out the optimal conditions that provide the largest modulator output eye-opening with the smallest I_{tail}, or the smallest power consumption. With a fixed value for R_L, larger I_{tail} generates larger output voltage swing but runs into the headroom problem if I_{tail} is too large. Fig. 3(c) shows simulated eye-diagrams at three different conditions, whose I_{tail} and R_L values are represented by Point A, B, C in Fig. 3(b). For the simulation, post-layout parasitic RC values for the driver are included as they can significantly influence the driver performance. Point A requires small I_{tail} for peak eye opening but experiences degradation due to large RC time constant as shown in the simulated eye-diagram. Point B and C show similar eye patterns but Point C requires larger I_{tail} due to smaller R_L, resulting in larger power consumption. Consequently, Point B provides the largest eye opening with the smallest power consumption. With such approach, the capability of simultaneous simulation of electronic circuits and photonic device should further enhance the potential of EPICs.

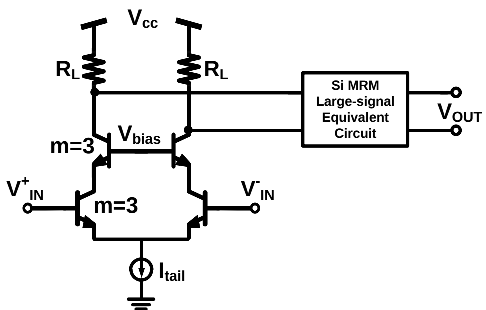

(a)

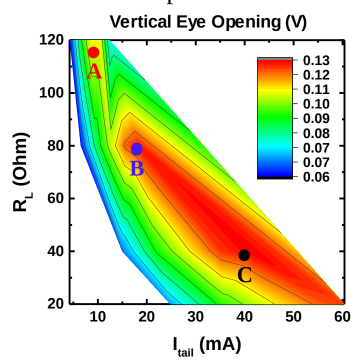

(b)

A (I_{tail} = 10.4mA) **B (I_{tail} = 18.4mA)** **C (I_{tail} = 41.3mA)**

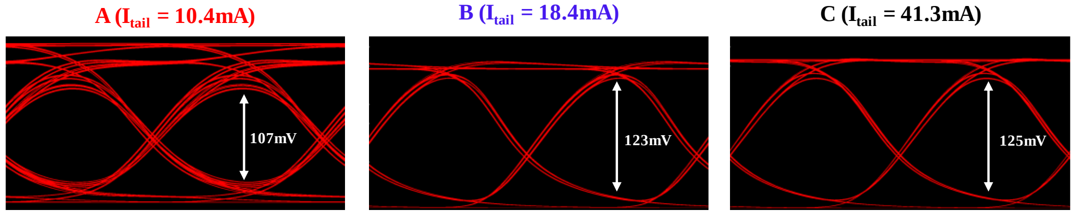

(c)

Fig. 3(a) Si Photonic transmitter based on Photonic BiCMOS technology, (b) Vertical eye opening for various R_L and I_{tail} values and (c) Simulated eye-diagrams at different I_{tail} and R_L combination.

4. Acknowledgement

This work was supported by National Research Foundation of Korea grant funded by the Korean Ministry of Science, ICT and Future Planning (2015R1A2A2A01007772) and Materials and Parts Technology R&D Program funded by the Korean Ministry of Trade, Industry & Energy (Project No. 10065666). Also, authors are thankful to IC Design Education Center (IDEC) for EDA tool support.

5. References

[1]P. Dong, S. Liao, D. Feng, H. Liang, D. Zheng, R. Shafiiha, C.-C. Kung, W. Qian, G. Li, X. Zheng, A. V Krishnamoorthy, and M. Asghari, "Low Vpp, ultralow-energy, compact, high-speed silicon electro-optic modulator," Opt. Express **17**, 22484–22490 (2009).

[2]G. Li, A. V Krishnamoorthy, I. Shubin, J. Yao, Y. Luo, H. Thacker, X. Zheng, K. Raj, and J. E. Cunningham, "Ring Resonator Modulators in Silicon for Interchip Photonic Links," IEEE J. Sel. Top. Quantum Electron. **19**, 95–113 (2013).

[3]R. Dube-Demers, J. St-Yves, A. Bois, Q. Zhong, M. Caverley, Y. Wang, L. Chrostowski, S. LaRochelle, D. V. Plant, and W. Shi, "Analytical Modeling of Silicon Microring and Microdisk Modulators With Electrical and Optical Dynamics," J. Light. Technol. **33**, 4240–4252 (2015).

[4]J. Rhim, Y. Ban, B.-M. Yu, J.-M. Lee, and W.-Y. Choi, "Verilog-A behavioral model for resonance-modulated silicon micro-ring modulator," Opt. Express **23**, 8762–8772 (2015).

[5]M. Shin, Y. Ban, B. M. Yu, M. H. Kim, J. Rhim, L. Zimmermann, and W. Y. Choi, "A Linear Equivalent Circuit Model for Depletion-Type Silicon Microring Modulators," IEEE Trans. Electron Devices **64**, 1140–1145 (2017).

[6]B. E. Little, S. T. Chu, H. A. Haus, J. Foresi, and J.-P. Laine, "Microring resonator channel dropping filters," J. Light. Technol. **15**, 998–1005 (1997).

[7]D. Knoll, S. Lischke, A. Awny, and L. Zimmermann, "(Invited) SiGe BiCMOS for Optoelectronics," ECS Trans. **75**, 121–139 (2016).